Bond Shift Rearrangement of Chloro-, Bromo-, and Iodobullvalene in the Solid State and in Solution. A Carbon-13 and Proton NMR Study

Z. Luz,*,† L. Olivier,† R. Poupko,† K. Müller,‡ C. Krieger,§ and H. Zimmermann§

Contribution from the Department of Chemical Physics, The Weizmann Institute of Science, Rehovot 76100, Israel, Institut für Physikalische Chemie, Universität Stuttgart, Pfaffenwaldring 55, D-7000 Stuttgart 80, Germany, and Max-Planck-Institut für Medizinische Forschung, A.G. Molekülkristalle, Jahnstrasse 29, 69120 Heidelberg, Germany

Received August 11, 1997

Abstract: The mechanisms of the Cope rearrangement in chloro-, bromo-, and iodobullvalene in solution and in the solid state were investigated by NMR techniques. The dominant species in solution, for all three compounds, are isomers 2 and 3 with nearly equal concentrations (where the numbers refer to the substituted carbons in the bullvalene moiety). The kinetics of the rearrangement processes as studied by ^{1}H and ^{13}C NMR involve three dominant bond shift rearrangements: interconversion between isomers 2 and 3, degenerate rearrangement of isomer 2, and a pseudodegenerate rearrangement of isomer 3, with isomer 1 serving as an intermediate. The solid state properties of these compounds were studied by carbon-13 MAS NMR and the bromo and iodo derivatives also by X-ray crystallography. Bromo- and iodobullvalene crystallize entirely as isomer 2 in the orthorhombic *Fdd*2 space group. The molecules in the crystals are orientationally disordered, and the carbon-13 results show that this disorder is dynamic on the NMR time scale. Rotor-synchronized two-dimension exchange spectroscopy, magnetization transfer experiments, and analysis of dynamic MAS spectra show that the mechanism of the dynamic disorder involves a degenerate rearrangement of isomer 2 which results in an effective π-flip of the molecule in the crystal. The Arrhenius activation parameters for this process are $\Delta E^{\dagger} = 57.1$ kJ/mol, $A = 5.2 \times 10^{12}$ s^{-1} for bromobullvalene and $\Delta E^{\dagger} = 58.5$ kJ/mol, $A = 1.8 \times 10^{13}$ s^{-1} for iodobullvalene. Chlorobullvalene is liquid at room temperature (mp 14 °C). Upon cooling of this compound in the MAS probe to well below 0 °C, signals due to both isomer 2 and isomer 3 are observed in the solid state. It is not known whether the solid so obtained is a frozen glass, a mixture of crystals due to, respectively, isomer 2 and isomer 3, or a single type of crystals consisting of a stoichiometric mixture of both isomers. Rotor-synchronized two-dimensional exchange measurements show that the chlorobullvalene isomers in this solid undergo Cope rearrangement. However, the bond shift processes involve only a degenerate rearrangement of isomer 2 and a pseudodegenerate rearrangement of isomer 3. No cross-peaks corresponding to interconversion between the two isomers are observed.

Introduction

The crystal structure and the dynamic properties of a number of solid monosubstituted bullvalenes, including those with X

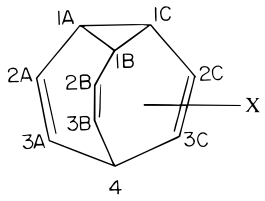

(1)

= F,[1] CN,[2] COOH,[2] SC_2H_5,[3] and bibullvalenyl,[4] were recently studied by X-ray diffraction and carbon-13 NMR. Although these compounds exist in solution in a dynamic equilibrium involving several substitutional isomers[5−10] in the solid state they all crystallize as a single isomer in well ordered lattices. Thus, fluorobullvalene crystallizes as isomer 4,[1] cyanobullvalene,[2] ethylthiobullvalene,[3] and bullvalene carboxylic acid[2] as isomer 3 and bibullvalenyl[4] as the 3−3 isomer (where the numbers labeling the isomers refer to the substitution site in eq 1 above). The interconversion between the isomers in solution involves the bond shift (Cope) rearrangement[11,12] via the cycle shown in Figure 1. According to this cycle isomer 4 can only rearrange to isomer 1, while isomer 3 can rearrange either to isomer 1 or to isomer 2. It came, therefore, somewhat as a surprise to find that the above monosubstituted bullvalenes also

† The Weizmann Institute of Science.
‡ Universität Stuttgart.
§ Max-Planck-Institut für Medizinische.

(1) Müller, K.; Zimmermann, H.; Krieger, C.; Poupko, R.; Luz, Z. *J. Am. Chem. Soc.* **1996**, *118*, 8006.
(2) Poupko, R.; Müller, K.; Zimmermann, H.; Krieger, C.; Luz, Z. *J. Am. Chem. Soc.* **1996**, *118*, 8015.
(3) Luger, P.; Roth, K. *J. Chem. Soc., Perkin Trans.* **1989**, *2*, 649.
(4) Olivier, L.; Poupko, R.; Zimmermann, H.; Luz, Z. *J. Phys. Chem.* **1996**, *100*, 17995.
(5) Schröder, G.; Oth, J. F. M. *Angew. Chem.* **1967**, *458*, 79.
(6) Oth, J. F. M.; Merenyi, R.; Nielsen, J.; Schröder, G. *Chem. Ber.* **1965**, *98*, 3385.
(7) Oth, J. F. M.; Merenyi, R.; Röttele, H.; Schröder, G. *Tetrahedron Lett.* **1968**, 3941.
(8) Hoogzand, C.; Nielsen, J.; Oth, J. F. M. *Tetrahedron Lett.* **1970**, 2287.
(9) Oth, J. M. F.; Machens, E.; Röttele, H.; Schröder, G. *Liebigs Ann. Chem.* **1971**, *745*, 112.
(10) Zwez, T. Ph.D. Dissertation, Karlsruhe University, 1988.
(11) Oth, J. F. M.; Müllen, K.; Gilles, J.-M.; Schröder, G. *Helv. Chim. Acta* **1974**, *57*, 1415.
(12) Poupko, R.; Zimmermann, H.; Müller, K.; Luz, Z. *J. Am. Chem. Soc.* **1996**, *118*, 7995.

S0002-7863(97)02802-3 CCC: $15.00
Published on Web 05/20/1998

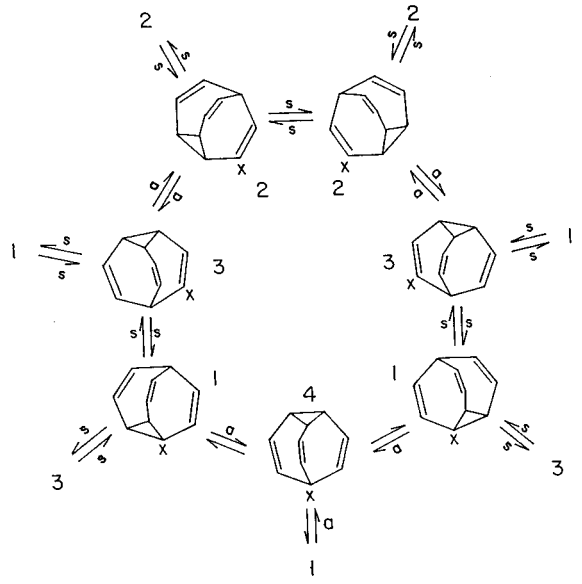

Figure 1. The bond shift isomerization cycle for monosubstituted bullvalenes. X is the substituent, and the isomers are labeled according to the substitution site. The letters a (anti) and s (syn) refer to whether a cyclopropane bond which is opposite (a) or next (s) to the substituted wing is cleaved during the process. The scheme shows that only isomer 2 can undergo a direct degenerate rearrangement, while isomer 3 can do so only via a short subcycle 3-[1]-3.

undergo Cope rearrangement in the solid state where they form well-ordered, single-isomer crystals. Using solid state NMR techniques, it was shown that the rearrangement in these solids proceeds via closed subcycles involving one or several isomers as short-lived intermediates. Moreover, to ensure that the rearranged molecules retain their proper orientation in the crystal, the rearrangement involves a concomitant reorientation.[1,2]

In the present work we extend the study to the three monosubstituted bullvalenes with X = Cl, Br, and I. These bullvalene derivatives differ from the previously mentioned homologues in several respects. While the latter exhibit in solution one major isomer in equilibrium with several minor species,[12] the chloro, bromo, and iodo derivatives exist in solution as an almost 1:1 mixture of isomers 2 and 3.[6,7,10] Their solid state properties are even more outstanding: thus, bromo- and iodobullvalene crystallize entirely as isomer 2, and although their crystals possess well defined positional order, they are orientationally disordered, with the molecules residing in lattice sites of symmetry higher then their own. Referring to Figure 1, we notice that isomer 2 is the only one which can undergo a direct degenerate interconversion. It is therefore of interest to check whether such a degenerate rearrangement occurs in solid bromo- and iodobullvalene and if it does, how it is related to the orientational disorder of the crystalline state.

We present X-ray measurements of the lattice structure of bromo- and iodobullvalene, and use carbon-13 magic angle spinning (MAS) NMR to identify the isomers constituting their crystals. Subsequently we apply 1D and 2D exchange NMR techniques to study the dynamics of the rearrangement processes in these solids as well as in a frozen sample of chlorobullvalene. The crystal structure of the latter compound (mp 14 °C) was not yet determined. The NMR results indicate that it solidifies as a mixture of isomers 2 and 3. However, so far we are unable to tell whether this solid corresponds to a thermodynamically stable crystalline form, a meta-stable solid, or a quenched glass.

For completeness we also investigated the kinetics of the rearrangement processes of all three systems in solution. Such measurements were performed earlier on bromobullvalene and a few other bullvalene derivatives by proton NMR at much lower frequencies.[6] Here we present a more complete study using both proton and carbon-13 NMR at high fields. We show that in all these cases three rearrangement processes dominate; interconversion of isomers 2 and 3, degenerate rearrangement of isomer 2, and a pseudodegenerate rearrangement of isomer 3 via the subcycle 3-[1]-3, with isomer 1 as an intermediate.

Experimental Section

The experimental details are as described in our previous publications on substituted bullvalenes,[1,12] except that some of the solid state NMR experiments were performed on a new Bruker DSX300 spectrometer and others on a high-resolution Bruker DMX500 equipped with a MAS probe.

The compounds were prepared as described in refs 6 and 7. As an example we describe in some detail the procedure used to synthesize

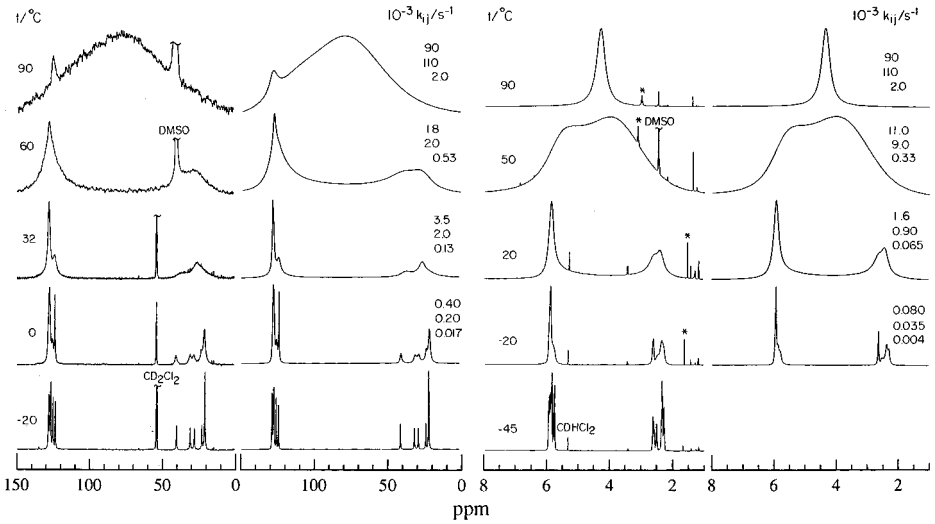

Figure 2. The left two columns show experimental and simulated dynamic carbon-13 NMR spectra of chlorobullvalene (at 100.6 MHz). The temperatures and solvents of the experimental spectra are indicated. The concentration of the solution was 0.3 M. The simulated spectra were calculated using the chemical shift parameters from Table 1 and the rate constants k_{23}, k_{22}, k^1_{33}, as indicated on the right-hand side, from top to bottom, respectively. The right two columns are similar results for ^{1}H NMR at 400 MHz. Asterisks indicate impurities. Spin−spin couplings were neglected in the calculations.

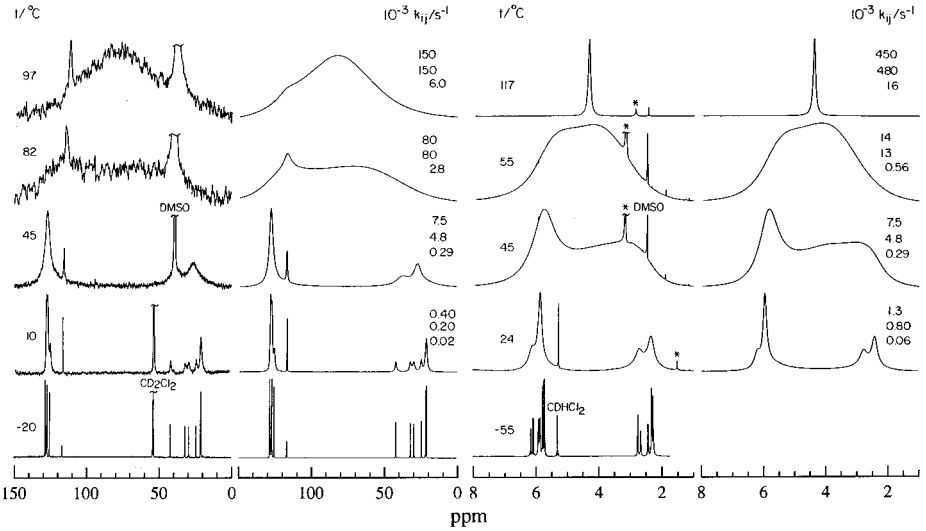

Figure 3. Same as in Figure 2, but for bromobullvalene (0.25 M). The carbon-13 and proton spectra were recorded at 125.7 and 500 MHz, respectively.

Table 1. ^{1}H and ^{13}C Chemical Shift Parameters and ^{13}C−^{1}H Spin−Spin Coupling Constants of Chloro-, Bromo-, and Iodobullvalene in Methylene Chloride Solutions[a]

	δ_C^{Cl}/ppm	δ_C^{Br}/ppm	δ_C^{I}/ppm	δ_H^{Cl}/ppm	δ_H^{Br}/ppm	δ_H^{I}/ppm	$^1J_{CH}^{Cl}$/Hz	$^1J_{CH}^{Br}$/Hz	$^1J_{CH}^{I}$/Hz
					Isomers 2				
1AB	20.56	21.31	22.26	2.35	2.36	2.29	167	167	165
1C	27.78	29.46	32.94	2.64	2.81	2.93	167	170	168
2AB	126.90	127.08	127.31	5.90	5.94	5.94	165	161	*a*
2C	127.43	116.87	91.10						
3AB	127.30	127.30	127.49	5.78	5.80	5.79	162	*a*	*a*
3C	123.58	127.77	136.42	5.89	6.16	6.49	167	167	169
4	30.49	31.98	34.15	2.52	2.47	2.27	132	134	133
					Isomers 3				
1AB	20.71	20.86	21.52	2.28	2.31	2.31	167	167	165
1C	22.63	24.38	26.76	2.34	2.34	2.25	168	169	169
2AB	128.41	128.56	128.64	5.95	5.98	6.00	159	*a*	160
2C	123.96	128.64	137.75	5.97	6.23	6.54	160	*a*	163
3AB	125.40	125.60	125.83	5.85	5.85	5.82	160	165	*a*
3C	128.70	116.71	88.02						
4	40.04	41.93	45.68	2.60	2.71	2.72	136	136	139

^{1}H−^{1}H, ^3J_i spin−spin coupling constants[b]

	$^3J_2^{Cl}$/Hz	$^3J_3^{Cl}$/Hz	$^3J_2^{Br}$/Hz	$^3J_3^{Br}$/Hz	$^3J_2^{I}$/Hz	$^3J_3^{I}$/Hz
1AB-1C	8.7	*a*	8.6	*a*	8.6	*a*
1C-2C		*a*		8.3		8.2
2AB-3AB	*a*	*a*	11.0	11.0	11.1	11.2
3AB-4	8.9	8.9	8.6	8.7	*a*	8.9
3C-4	8.9		9.4		9.4	

[a] Could not be measured. [b] The subscripts i refers to the isomers 2 or 3.

chlorobullvalene. To a solution of bullvalene (7.5 g) in chloroform (20 mL) was slowly added 5.4 mL of sulfuryl chloride (SO_2Cl_2) while stirring, followed by refluxing for exactly 30 min. After cooling the solvent was allowed to evaporate, and the oily dichlorobullvalene residue crystallized in a freezer. After recrystallization from *n*-hexane the dichloride intermediate (2.5 g) had a melting point of 116−118 °C. Conversion of the dichloro derivative to monochlorobullvalene was affected by elimination of HCl using potassium-*tert*-butylate (prepared from 5.2 g of potassium and 130 mL of *tert*-butyl alcohol): Five grams of the dichlorobullvalene were refluxed in the alcoholate solution overnight. The solvent was then removed by a rotavapor, and the residue distilled under reduced pressure (10^{-3} Torr) in a bulb tube. The monochlorobullvalene distillate was purified by chromatography (silica, CH_2Cl_2:*n*-hexane 6:4) followed by a second vacuum distillation to yield 1.3 g of the desired compound. Combustion analysis: exp%-(calc%), C:73.24(72.96), H: 5.63(5.51), Cl: 21.73(21.53).

Results and Discussion

A. The Isomeric Equilibria and Interconversion Kinetics in Solution. The high-resolution proton and carbon-13 NMR spectra of chloro-, bromo-, and iodobullvalene in solution at low temperatures (< −30 °C for carbons-13, and < −50 °C for protons) exhibit peaks due solely to isomers 2 and 3 (see bottom spectra in Figures 2−4).[6,7,10] The magnetic parameters of these isomers (^{1}H and ^{13}C chemical shifts and spin spin coupling constants) are summarized in Table 1. The peak assignment was established by several experiments, including ^{13}C−^{1}H correlation and 2D exchange spectroscopy. Wherever comparable, the results are consistent with previous assignments.[10] From these low-temperature spectra the equilibrium concentration ratios, $K = P_3/P_2$, of isomers 3 and 2, could be determined from the spectral peak intensities. The results so

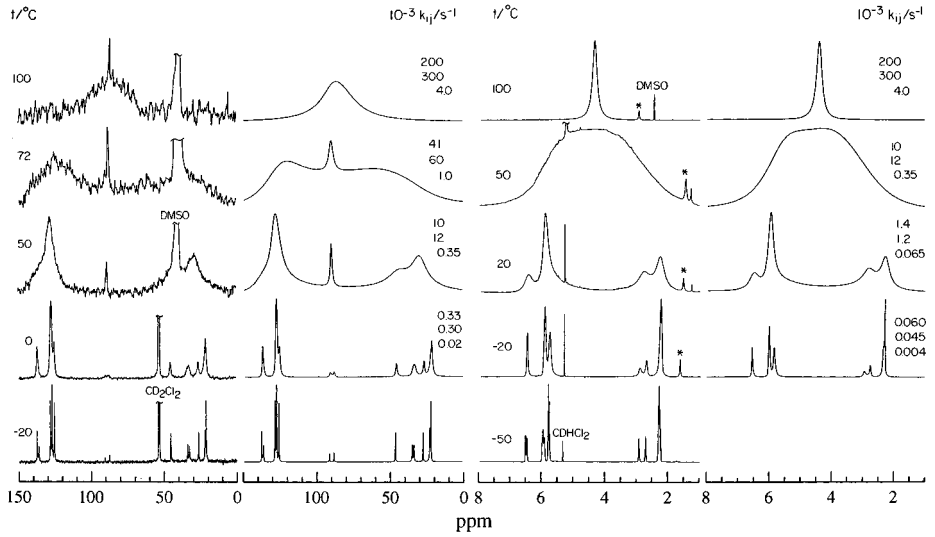

Figure 4. Same as in Figure 2, but for iodobullvalene (0.2 M).

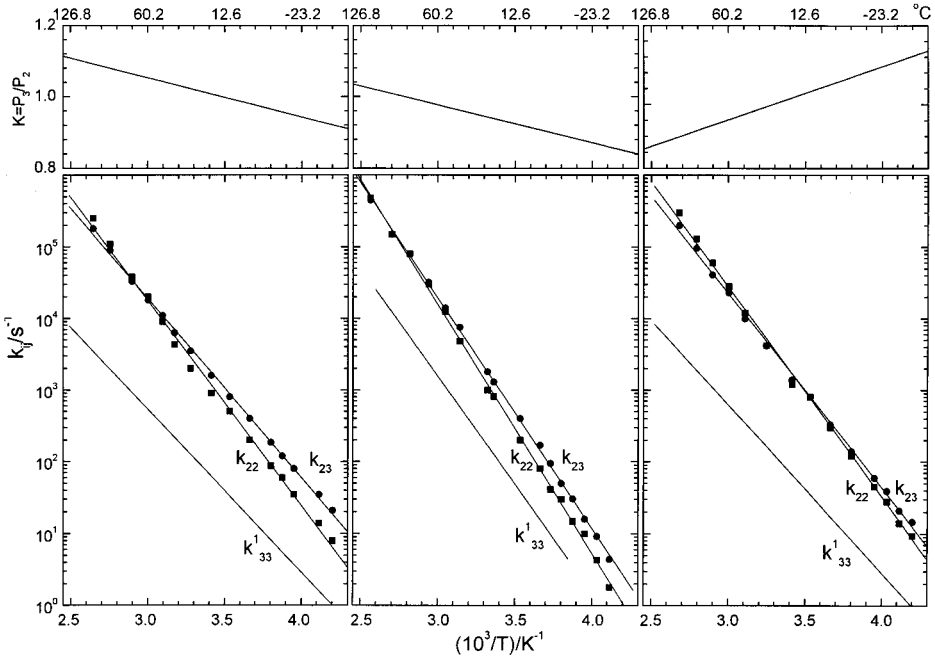

Figure 5. Arrhenius plots for k_{23}, k_{22}, and k^1_{33} (bottom), and the equilibrium constants, $K = P_3/P_2$ (top), for chloro- (left), bromo- (middle), and iodobullvalene (right) in solution.

obtained (and extrapolated to higher temperatures) are plotted in the upper parts of the diagrams in Figure 5. It may be seen that for all three compounds, $K = 1 \pm 0.15$ in the temperature range −50 to 140 °C. It is interesting, however, that while K decreases upon heating for iodobullvalene, it has an opposite temperature dependence for the chloro and bromo derivatives.

As the temperature is raised to above −40 °C, line broadening sets in due to bond shift isomerism (see Figures 2−4). The general behavior for the three compounds is quite similar. Therefore we shall describe in some detail the analysis of one homologue, i.e., bromobullvalene, and then only give a summary of the results for the chloro and iodo derivatives.

If we consider only isomers 3 and 2 the isomerization scheme of Figure 1 leads to the exchange matrix shown in Table 2. The rows and columns in this matrix label the carbons (hydrogens) in the various isomers (indicated as superscripts), while the k_{ij}'s are the rate constants for the isomerization of isomer j to isomer i. The direct interconversion between isomers 3 and 2 can be schematically represented by the diagrams where

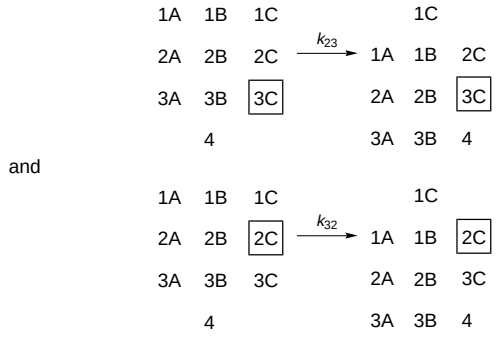

(2)

the symbols represent the carbons or hydrogens in the structural formula shown in eq 1 and the squares indicate the substitution sites. This process leads to the k_{23} and k_{32} entries in the exchange matrix of Table 2. In the fast exchange regime this reaction should result in a set of seven peaks [($1AB^2$, $3AB^3$); ($2AB^2$, $2AB^3$); ($3AB^2$, $1AB^3$); ($1C^2$, 4^3); ($3C^2$, $2C^3$); (4^2, $1C^3$)

Chart 1

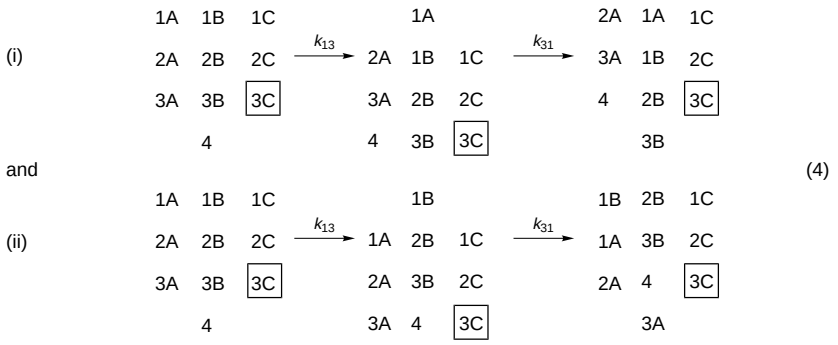

Table 2. The Exchange Matrix Used To Simulate the Solution Spectra of Chloro-, Bromo-, and Iodobullvalene[a]

	$1AB^3$	$2AB^3$	$3AB^3$	$1C^3$	$2C^3$	$3C^3$	4^3	$1AB^2$	$2AB^2$	$3AB^2$	$1C^2$	$2C^2$	$3C^2$	4^2
$1AB^3$	$-k_{23}-{}^1/_2k^1_{33}$	${}^1/_2k^1_{33}$								k_{32}				
$2AB^3$	${}^1/_2k^1_{33}$	$-k_{23}-k^1_{33}$	${}^1/_2k^1_{33}$						k_{32}					
$3AB^3$		${}^1/_2k_{33}$	$-k_{23}-k^1_{33}$				k^1_{33}	k_{32}						
$1C^3$				$-k_{23}$										k_{32}
$2C^3$					$-k_{23}$								k_{32}	
$3C^3$						$-k_{23}$						k_{32}		
4^3			${}^1/_2k^1_{33}$				$-k_{23}-k^1_{33}$				k_{32}			
$1AB^2$			k_{23}					$-k_{32}-k_{22}$		${}^1/_2k_{22}$				k_{22}
$2AB^2$		k_{23}							$-k_{32}-{}^1/_2k_{22}$	${}^1/_2k_{22}$				
$3AB^2$	k_{23}							${}^1/_2k_{22}$	${}^1/_2k_{22}$	$-k_{32}-k_{22}$				
$1C^2$							k_{23}				$-k_{32}-k_{22}$		k_{22}	
$2C^2$						k_{23}						$-k_{32}$		
$3C^2$					k_{23}						k_{22}		$-k_{32}-k_{22}$	
4^2				k_{23}				${}^1/_2k_{22}$						$-k_{32}-k_{22}$

[a] The k_{ij} are rate constants as defined in the tex.

and ($2C^2$, $3C^3$)] in the carbon-13 spectrum or just six multiplets in the proton spectrum (since there are no $2C^2$ and $3C^3$ protons). In practice, however, at high temperatures the whole proton spectrum coalesces to a single sharp peak (at 4.36 ppm), while the carbon spectrum exhibits a narrow peak due to the coalesced signal $2C^2$, $3C^3$ (in the range 113−116 ppm) and a broad band due to the rest of the carbons (see Figure 3).

This behavior indicates the occurrence of additional isomerization processes, the most likely one being the degenerate rearrangement of isomer 2. This process can proceed through two possible pathways, depending on which of the neighboring (syn) cyclopropane bonds is cleaved

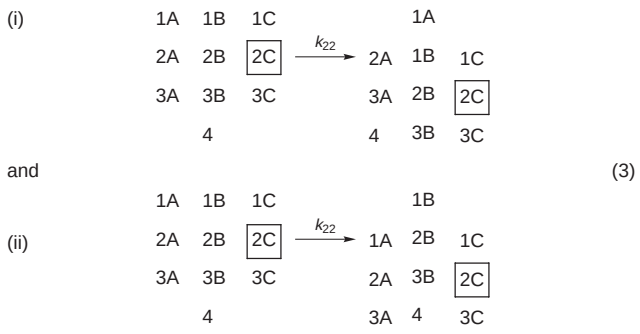

Assuming equal probability for both pathways this process leads to the k_{22} entries in Table 2. The part of the exchange matrix due to isomer 2 is thus factorized into three blocks due, respectively, to the $1AB^2$, $2AB^2$, $3AB^2$, and 4^2 carbons, the $1C^2$ and $3C^2$ carbons, and the isolated $2C^2$ atom.

Examination of the carbon-13 spectra shows that the coalesced $2C^2/3C^3$ peak, after undergoing exchange narrowing at around 10 °C, broadens up to a maximum width of about 300 Hz at 75 °C and then it narrows again down to 50 Hz at 120 °C. Concomitantly it undergoes a shift to high field of about 350 Hz. These changes in the width and shift of the $2C^2/3C^3$ peak are plotted in Figure 6. This behavior suggests the presence of an additional isomeric species in dynamic equilibrium with isomers 3 and 2, whose concentration is, however, too low to detect, at least at low temperature, before line broadening sets in. The most likely species responsible for this effect is isomer 1, via the subcycle $3 \xrightarrow{k_{13}} [1] \xrightarrow{k_{31}}$. There are two pathways for this mechanism that lead to permutation between atoms. These are shown in Chart 1.

Assuming equal probability for the two pathways and an infinitesimal concentration of isomer 1, the effect of this mechanism on the carbon-13 and proton NMR line shape can be taken into account as indicated by the k^1_{33} entries in the exchange matrix (Table 2), with $k^1_{33} = {}^1/_2k_{13}$.[1,4] The dynamic line shape thus depends on three rate constants, k_{23}, k_{22}, and k^1_{33} and the equilibrium ratio $K = k_{32}/k_{23}$. In practice, k^1_{33} was initially estimated from the results of Figure 6 and then refined together with k_{22} and k_{23} by simultaneously fitting the experimental proton and carbon-13 line shapes using the full exchange matrix of Table 2. Examples of such simulated spectra are shown in the second and fourth columns of Figure 3. Note that the exchange matrix does not include the effect of the intermediate isomer 1 (eq 4) on the coalesced $2C^2/3C^3$ carbon-13 signal. For the simulation we added an effective line width to this peak equal to $k_{13} = 2k^1_{33}$. This is a reasonable approximation up to the temperature at which this peak reaches its maximum width; thereafter the approximation breaks down. However, this deficiency does not cause a serious error in determining the various rate constants by fitting the overall line shapes. From the analysis of the results in Figure 6 we estimate

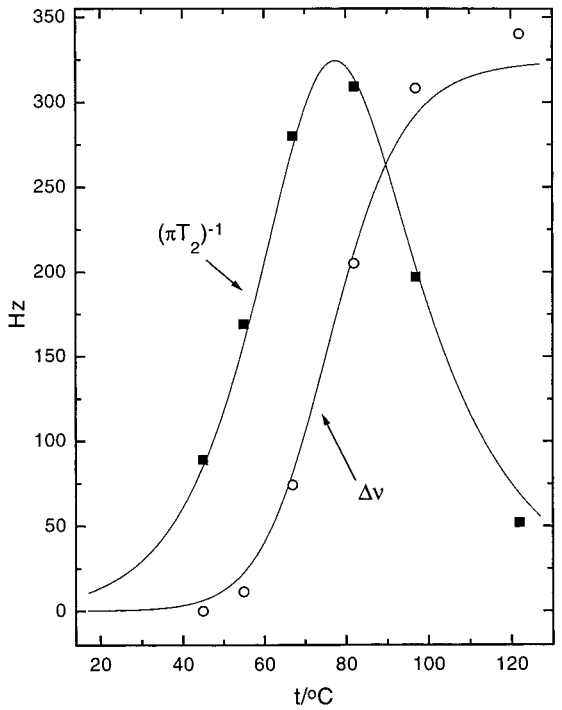

Figure 6. The full line width $1/\pi T_2$, and the frequency shift, $\Delta\nu$, of the coalesced $2C^2/3C^3$ carbon-13 peak in bromobullvalene as function of temperature. $\Delta\nu$ is the upfield shift, measured from the peak position at 20 °C. The full lines are calculated for the rate constants plotted in Figure 5 with an estimate chemical shift of 25 ppm and a fractional population of $P_1 = 0.057$ for isomer 1.

a fractional concentration $P_1 = 0.057$ for isomer 1 at 75 °C.[1,4] Its concentration is, however, expected to decrease upon cooling, thus explaining its undetectibility in the low temperatures NMR spectra. The overall kinetic results are summarized in the middle part of Figure 5 in terms of Arrhenius plots for the three rate constants.

The solution spectra of chloro- and iodobullvalene (Figures 2 and 4) were analyzed in much the same way, and the corresponding kinetic and thermodynamic results are included in Figure 5. The relevant parameters for all compounds (including the estimated error) are also summarized in Table 3. In general these results are in agreement with the earlier study of Oth et al.[6] In particular the relative importance of the k_{ij}'s and, for bromobullvalene, also the estimated average rearrangement rate (at 80 °C) given by these authors is similar to that determined here. The present analysis is, however, considerably more extensive and provides separate kinetic parameters for the various bond shift mechanisms.

B. The Crystal Structure of Bromo- and Iodobullvalene. The melting temperatures and (in brackets) the melting enthalpies of chloro-, bromo-, and iodobullvalene are, respectively, 14 °C (13.5 kJ/mol), 44 °C (14.2 kJ/mol), and 103 °C (15.5 kJ/mol). All three compounds undergo pronounced supercooling (40−50 K at 5 K/min). The indicated melting temperatures and enthalpies were obtained by differential scanning calorimetry upon heating. The transition peaks were always sharp and the data highly reproducible (see below, however, for some comments concerning chlorobullvalene). For comparison, unsubstituted bullvalene melts at 96 °C (16.0 kJ/mol) and supercools much less (∼20 K).

Since chlorobullvalene is liquid at room-temperature we were unable to determine its structure. Both the bromo and iodo derivatives crystallize as colorless needles in the orthorhombic *Fdd2* space group, with unit cell dimensions as shown in Table 4. In both crystals there are eight molecules per unit cell, located on crystallographic C_2 symmetry axes. Since none of the monosubstituted isomers of bullvalene can have a molecular C_2 symmetry axis, this result indicates that both compounds form orientationally disordered crystals. Because of this disorder we were not able to determine from the X-ray results which isomer(s) constitute the crystal lattices. Since in solution these compounds exist as a mixture of isomers 2 and 3 with nearly equal concentrations, it is even difficult to guess; it could be that the crystals consist of both isomers 2 and 3 or of just one of the two.

C. Carbon-13 MAS NMR at Low Temperatures. Fortunately the isomeric species which make up the crystals could readily be determined from the carbon-13 MAS spectra at low temperatures. Such spectra for the three bullvalene homologues studied are shown in Figure 7. The figure also gives the peak assignment of the center bands, as determined by comparison with the isotropic chemical shifts in the solution spectra of the corresponding compounds. In the spectra of crystalline bromo- and iodobullvalene only peaks due to isomer 2 are assigned. This is based on the complete absence of peaks due to carbons 4^3 and $1C^3$ in the experimental MAS spectra. In solution these peaks are well isolated from the rest of the signals (cf. Figures 3 and 4) and should have been clearly observed in the MAS spectra, had isomer 3 been present in the solids. We thus conclude that bromo- and iodobullvalene crystallize entirely as isomer 2, and based on the crystallographic results described in the previous section the molecules must be assumed to be orientationally disordered with an average C_2 symmetry. We shall see below that this disorder is dynamic with the switching between the two orientations coupled via the Cope rearrangement.

The situation is quite different for chlorobullvalene. The solid state carbon-13 MAS spectra in this case were obtained by cooling the liquid compound within the spinning sample holder to below the freezing temperature. The resulting spectrum at −43 °C is shown in the top trace of Figure 7. In this case, signals due to both isomers 2 and 3, with nearly equal intensity, are observed. However, because of lack of crystallographic information on this compound, we know very little about the nature of this solid. It could be a thermodynamically stable crystal consisting of a 1:1 stoichiometric ratio of isomers 2 and 3, or it could be a mixture of two crystallographic forms, one containing isomer 2 and the other containing isomer 3, or perhaps a solid glass obtained by quenching the liquid chlorobullvalene, while retaining the equilibrium concentrations of the two isomers as in the liquid. We shall see in a subsequent section that chlorobullvalene undergoes bond shift rearrangement in this solid, although for both isomers the rearrangement is degenerate (or pseudodegenerate) in the sense that isomer 2 rearranges only to itself and likewise isomer 3.

For the quantitative interpretation of the dynamic spectra to be described in the next section we need to know the anisotropic chemical shift tensors for the various carbons of the bullvalene compounds. These were determined from the spinning sideband intensities of the low-temperature spectra, using the method of Herzfeld and Berger.[13] The results are summarized in Table 5. Only data for the olefinic carbons are given. The chemical shift anisotropy for the aliphatic carbons is too small to affect the dynamic MAS at the spinning rates used in our experiments. The corresponding principal directions were assumed on the basis of molecular structure considerations as described previously.[1,14] They are indicated in Figure 8.

(13) Herzfeld, J.; Berger, A. E. *J. Chem. Phys.* **1980**, *73*, 6021.
(14) Luz, Z.; Poupko, R.; Alexander, S. *J. Chem. Phys.* **1993**, *99*, 7544.

Table 3. Equilibrium and Kinetic Parameters for the Various Bond Shift Processes in Solutions of Chloro-, Bromo-, and Iodobullvalene[a,b]

A. Equilibrium Parameters

X	K_0	ΔE (kJ/mol)
Cl	1.47	−0.93
Br	1.38	−0.98
I	0.64	1.14

B. Kinetic Parameters

X	k_{23} (300 K) (s^{-1})	A_{23} (s^{-1})	$\Delta E^{\dagger}_{23}$ (kJ/mol)	$\Delta S^{\dagger}_{23}$ (eu)	k_{22} (300 K) (s^{-1})	A_{22} (s^{-1})	$\Delta E^{\dagger}_{22}$ (kJ/mol)	$\Delta S^{\dagger}_{22}$ (eu)	k^1_{33} (300 K) (s^{-1})	A^1_{33} (s^{-1})	$\Delta E^{\dagger}_{33}$ (kJ/mol)	$\Delta S^{\dagger}_{33}$ (eu)
Cl	2.6×10^3	5.18×10^{11}	47.7 ± 3.8	-6.9 ± 3.0	1.7×10^3	1.49×10^{13}	57.1 ± 3.2	-3.0 ± 2.5	95	4.10×10^9	43.8 ± 3.0	-16.5 ± 3.0
Br	1.6×10^3	4.65×10^{13}	60.1 ± 4.1	2.0 ± 3.3	1.0×10^3	2.65×10^{14}	65.6 ± 4.0	5.5 ± 3.7	78	8.25×10^{11}	57.6 ± 6.3	-6.0 ± 4.0
I	2.7×10^3	2.84×10^{12}	51.8 ± 5.0	-3.6 ± 4.4	3.0×10^3	2.08×10^{13}	56.7 ± 4.6	1.1 ± 4.0	108	6.04×10^9	44.5 ± 4.7	-15.8 ± 4.0

[a] $K = P_3/P_2 = k_{32}/k_{23} = K_0 \exp(\Delta E/RT)$. [b] $k_{ij} = A_{ij} \exp(-\Delta E^{\dagger}_{ij}/RT) = (ek_BT/h) \exp(\Delta S_{ij}{}^{\dagger}/R) \exp(-\Delta H_{ij}{}^{\dagger}/RT)$.

Table 4. Unit Cell Dimensions of Bromo- and Iodobullvalene[a]

X	*a*/Å	*b*/Å	*c*/Å
Br	11.643 (5)	18.286 (4)	8.019 (5)
I	11.657 (3)	18.476 (4)	8.309 (2)

[a] Orthorhombic system. Space group *Fdd*2 (#43). Eight molecules per unit cell.

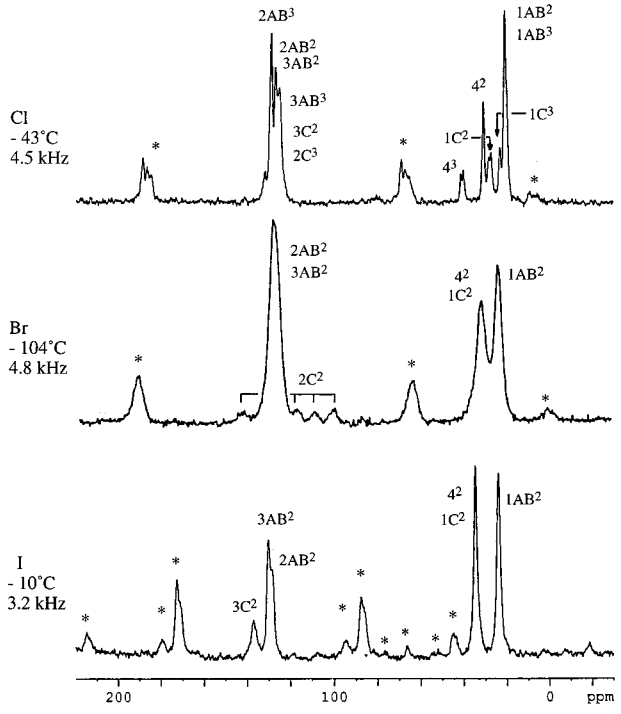

Figure 7. Solid state, carbon-13 MAS spectra at 75.46 MHz of chloro- (top), bromo- (middle), and iodobullvalene (bottom) at the indicated temperatures and spinning rates. The assignment of the center peaks are given; sidebands are marked by asterisks.

Finally we comment on the structure of the spectrum which was assigned to the $2C^2$ carbon of bromobullvalene (middle trace in Figure 7). It comprises of an asymmetric quartet as indicated in the figure. Such spectra have been observed before in MAS experiments of carbons bonded to quadrupole nuclei with spins $I = 3/2$.[15−20] The splitting results from the residual dipolar and indirect interactions between the carbon and adjacent quadrupolar nuclei, which are not averaged by the MAS. Spectra similar to that observed for the $2C^2$ carbon of bromobullvalene were, for example, observed in bromouracil[17] and in 1,3,5-tribromobenzene.[19] We were able to analyze this spectrum using eqs 13 and 14 or [1,2] of the first and second paper of ref 20, respectively. These equations apply for the situation in which the ^{79,81}Br quadrupole interactions $^{79,81}\chi = e^2qQ/h$ are much larger than their Larmor frequencies $^{79,81}\nu_{Br}$ and under the assumption that the quadrupole coupling tensors,

Table 5. The Principal Values of the Carbon-13 Chemical Shift Tensors (δ), the Line Width ($\Delta = 1/\pi T_2$) and Cross Polarization Efficiency (CP_{eff}) Assumed in the Simulation of the Dynamic MAS Spectra, for Iodo-, Bromo-, and Chlorobullvalene

Iodobullvalene: (Isomer 2)

I	δ_{iso}/ppm	δ_{xx}/ppm	δ_{yy}/ppm	δ_{zz}/ppm	Δ/Hz	CP_{eff}
$1AB^2$	23.7				130	1
$1C^2$	34.75				120	0.85
$2AB^2$	128.2	85	8	−93	155	1
$3AB^2$	129.94	85	8	−93	120	1
$3C^2$	137	86	5	−91	190	1
4^2	34.55				120	0.85

Bromobullvalene: (Isomer 2)

Br	δ_{iso}/ppm	δ_{xx}/ppm	δ_{yy}/ppm	δ_{zz}/ppm	Δ/Hz	CP_{eff}
$1AB^2$	22.5				200	1
$1C^2$	31				200	0.8
$2AB^2$	128	94	−6	−88	260	1
$3AB^2$	128	94	−6	−88	260	1
$3C^2$	128	94	−6	−88	260	1
4^2	32				200	0.8

Cl	δ_{iso}/ppm	δ_{xx}/ppm	δ_{yy}/ppm	δ_{zz}/ppm
Chlorobullvalene: (Isomer 2)				
$1AB^2$	21			
$1C^2$	27.8			
$2AB^2$	126.9	90	0	−90
$3AB^2$	126.9	90	0	−90
$3C^2$	123.6			
4^2	31.1			
Chlorobullvalene: (isomer 3)				
$1AB^3$	21			
$1C^3$	23.4			
$2AB^3$	128.9	93	2	−95
$3AB^3$	125.1	72	29	−101
$2C^3$	124			
4^3	40.9			

(15) Harris, R. K.; Olivieri, C. *Prog. NMR Spectrosc.* **1992**, *24*, 435.
(16) Harris, R. K.; Sünneçioglu, M. M.; Cameron, K. S.; Riddell, F. G. *Magn. Reson. Chem.* **1993**, *31*, 963.
(17) Nagasaka, B.; Takeda, S.; Nakamura, N. *Chem. Phys. Lett.* **1994**, *222*, 486.
(18) Alarcón, S. H.; Olivieri, A. C.; Carss, S. A.; Harris, R. K.; Zuriaga, M. J.; Monti, G. A. *J. Magn. Reson.* **1995**, *116A*, 244.
(19) Aliev, A. E.; Harris, K. D. M.; Harris, R. K.; Carss, S. A.; Olivieri, A. C. *J. Chem. Soc., Faraday Trans.* **1995**, *91*, 3167.
(20) Olivieri, A. C. *J. Magn. Reson.* **1993**, *101A*, 313; Alarcon, S. H.; Olivieri, A. C.; Carss, S. A.; Harris, R. K. *Magn. Reson. Chem.* **1995**, *33*, 603.

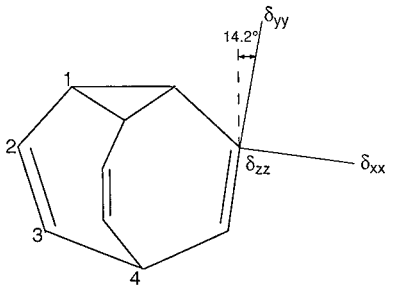

Figure 8. Assumed principal directions of the chemical shift tensors for the various types of carbons in the bullvalene moiety.

the bromine−carbon anisotropic indirect spin−spin couplings $^{79,81}\Delta J$, and the direct dipolar interactions $^{79,81}D = \gamma_C\gamma_{Br}h/4\pi^2r^3_{C-Br}$ are all axially symmetric and collinear with the Br−C bond direction. In practice, because of the low resolution of the spectrum, we used average values for the magnetic parameters of the two bromine isotopes. Assigning the outer and inner doublets of the asymmetric quartet to, respectively, the bromine $\pm 3/2$ and $\pm 1/2$ states, and taking D and χ to be positive, we obtained the following estimates for the relevant (average) parameters: $D' = D - \Delta J/3 = 964$ Hz, $J = -200$ Hz, $\delta^{Br}_{2C^2} = 117.25$ ppm, $\chi = 405$ MHz with $R = \chi/\nu_{Br} = 5.2$. These results are quite reasonable; the chemical shift is nearly the same as in solution (116.87 ppm), and the J and χ values are comparable to those determined for similar bromine compounds.[17,19] If we assume that r_{C-Br} is as in the related compound methyl-4-bromo-5-oxobicyclo[4.2.1]non-3-ene-1-carboxylate (1.91 Å)[21] we can estimate an average value for D (1128 Hz) and from this and D' calculate ΔJ to be 492 Hz. This is probably the least accurate result, because it is calculated as a (small) difference of relatively large numbers. It is nevertheless similar to that determined for the bromine bonded carbon in bromouracil (+210 Hz).[17]

With increasing temperature from −104 °C, the $2C^2$ multiplet gradually broadens resulting at −20 °C in a broad hump. We attribute this broadening to quadrupole relaxation effects of the bromine nucleus. At higher temperatures the $2C^2$ signal is smeared out by the general broadening of the spectrum due to the exchange process discussed below.

No resolved peaks were detected for the $2C^2$ carbon in the MAS spectra of iodobullvalene, most likely due to relaxation effects. Likewise no signals due to the $2C^2$ and $3C^3$ carbons were observed in the MAS spectrum of the solidified chlorobullvalene. The effect of the quadrupole chlorine nuclei is, however, clearly seen on the signals of the neighboring carbons, 4^3 of isomer 3 and $1C^2$ of isomer 2. Both signals show splittings (see Figure 7) characteristic of quadrupole interaction effects. When recorded at a higher frequency (see section E below) this splitting coalesces and a sharp peak is observed for both signals.

D. Dynamic Carbon-13 MAS Spectra of Bromo- and Iodobullvalene. The carbon-13 MAS spectra of bromo and iodobullvalene, above about 0 °C, exhibit line broadening that may clearly be attributed to dynamic effects (see Figure 9). The

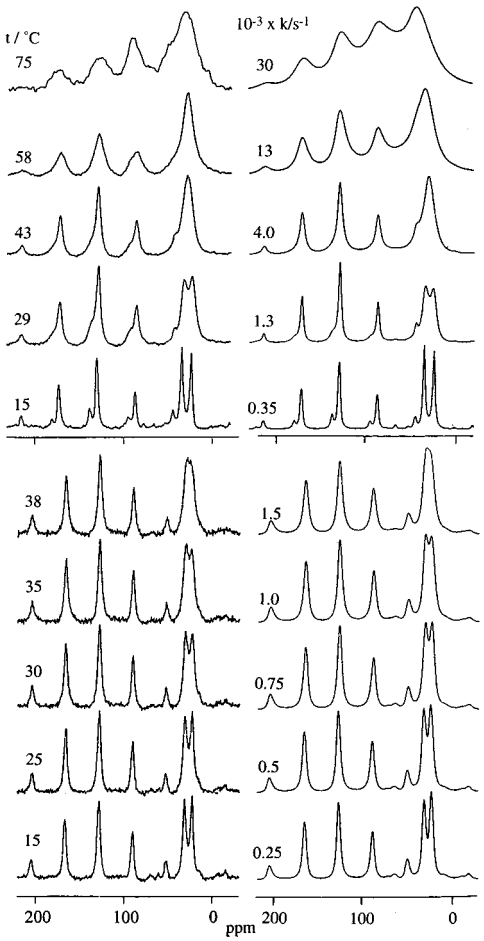

Figure 9. Experimental (left) and calculated (right) dynamic MAS carbon-13 spectra (at 75.46 MHz) of bromo (bottom set of spectra) and iodobullvalene (upper set of spectra). The temperatures at which the experimental spectra were recorded and the rate constants, k_c, used in the calculations are indicated. The spinning rates were 2.8 kHz for the bromo and 3.2 kHz for the iodo derivatives.

temperature range over which these measurements were carried out (up to 38 °C for the bromo and up to 95 °C for the iodo derivatives) was limited by the melting points of the compounds. The dynamic line shapes are therefore restricted to the slow exchange regime where detailed information about the reaction mechanism is more difficult to extract. Three types of processes may be imagined to be responsible for the observed dynamic effects in the MAS spectra. They are schematically illustrated in Figure 10. Recalling that the crystals are orientationally disordered one possibility is that the exchange involves pure molecular π-flips about the crystallographic C_2 axes. To conform with this picture we shall assume that the C-wings, which include the substituent, lie parallel to the C_2 axes and that the pseudo 3-fold symmetry axes of the bullvalene moieties lie perpendicular to these axes. The dynamic disorder process under these conditions is shown in Figure 10a and the corresponding exchange matrix is depicted in Table 6a. The rows and columns in this matrix label the $9 \times 2 = 18$ different carbon sites of the two molecules, with one set primed and the corresponding set unprimed. The matrix thus factorizes into nine 2×2 blocks. The $2C^2$ carbons are not included in the matrix since their signal is not observed in the carbon-13 MAS spectrum. The isotropic chemical shift of the primed and corresponding unprimed carbons are identical, but their anisotropic tensors, although congruent, are in general tilted with respect to each other. Hence jumps between the two orientations

(21) Kraus, W.; Partzelt, H.; Saldo, H.; Savitzky, G.; Schweiger, G. *Liebigs Ann. Chem.* **1981**, 1826.
(22) Kentgens, A. P. M.; de Jong, A. F.; de Boer, E.; Veeman, W. S. *Macromolecules* **1985**, *18*, 1045. Kentgens, A. P. M.; de Boer, E.; Veeman, W. S. *J. Chem. Phys.* **1987**, *87*, 6859.
(23) Hagemeyer, A.; Schmidt-Rohr, K.; Spiess, H. W. *Adv. Magn. Reson.* **1989**, *13*, 85.
(24) Luz, Z.; Spiess, H. W.; Titman, J. J. *Isr. J. Chem.* **1992**, *32*, 145.
(25) Titman, J. J.; Luz, Z.; Spiess, H. W. *J. Am. Chem. Soc.* **1992**, *114*, 3756.
(26) Schmidt, A.; Vega, S. *J. Chem. Phys.* **1987**, *87*, 6895.
(27) Schlick, S.; Luz, Z.; Poupko, R. *J. Am. Chem. Soc.* **1992**, *114*, 4315.

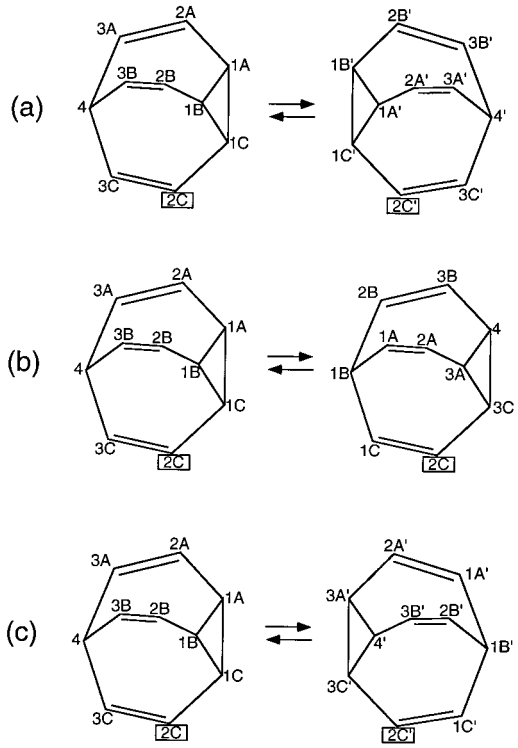

Figure 10. Schematic representation of the three dynamic processes considered for isomer 2 of monosubstituted bullvalene in an orientational disordered lattice. It is assumed that the pseudo-3-fold axis of the bullvalene moiety is perpendicular to a crystallographic C_2 axis (in a vertical direction) and that wing C with the substituent (2C) is in the plane of the figure. Mechanism a (top) corresponds to a pure π-flip about C_2. Mechanism b (middle) corresponds to a degenerate 2−2 rearrangement/reorientation which preserves the original orientation of the molecule. Mechanism c (bottom) corresponds to a degenerate 2−2 rearrangement which does not preserve the original molecular orientation. This process couples the orientation disorder with the Cope rearrangement. For (b) and (c) only one of two possible pathways is indicated.

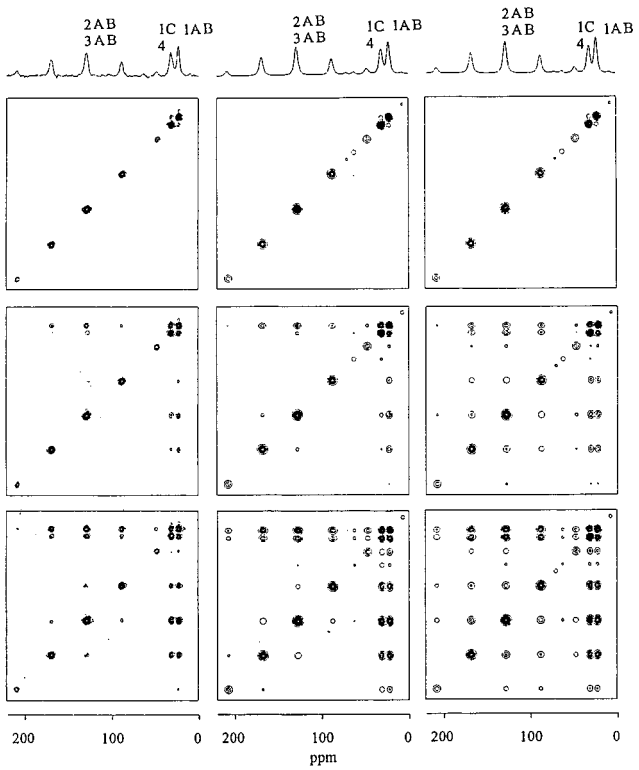

Figure 11. Rotor-synchronized carbon-13 two-dimensional exchange spectra of solid bromobullvalene at 75.46 MHz. Left column: Experimental spectra recorded at −25 °C with a spinning rate of 3.0 kHz for (from top to bottom) mixing times of 0.01, 0.1, and 0.5 s. Phase sensitive, experiments were performed as described in refs 23−25. Sixty-four increments at intervals of 33.3 μs were recorded in the t_1 domain. The number of scans for each t_1 increment was 24 (six for each of the four basic sequences). Recycle time, 10 s. Exponential line broadening, 35 Hz. Middle and right columns: Simulated spectra for mechanisms c and b, respectively (see Figure 10 and Table 6), for (from top to bottom) $k_\alpha\tau_m$ values of 0.1, 1, and 5, where $\alpha \equiv$ c or b.

will lead to line broadening in the MAS spectrum (although not to coalescence of lines as would be expected for a rearrangement reaction).

The bond shift cycle of Figure 1 shows that isomer 2, which is the prevailing isomer in solid bromo and iodobullvalene, can undergo a degenerate rearrangement of the type $2 \rightleftarrows 2$ and is therefore also likely to occur in these solids. Schemes (b) and (c) of Figure 10, describe such a rearrangement. However, while in (b) the rearrangement is coupled with a reorientation step which reverts the molecule to its original orientation in the crystal (as would necessarily be the case in an ordered crystal), scheme (c) corresponds to a situation in which the rearrangement results in the bullvalene moiety flipped with respect to its original orientation. Such a process is allowed because of the orientational disorder of the crystal. As discussed for the solution results, the degenerate $2 \rightleftarrows 2$ rearrangement can follow two pathways depending on whether the bond shift involves the 1,5 diene systems 3A, 2A, 1A, 1C, 2C, 3C (i) or 3B, 2B, 1B, 1C, 2C, 3C (ii) (see Chart 2).

The first step in these diagrams, indicated by 2−2, represents a rearrangement without molecular flip and thus to case (c) of Figure 10, while the second step, indicated by C_2, restores the original orientation. If this step is included, the situation applies to case (b). Note that in Figure 10(c) only the second pathway (ii) is indicated. Assuming equal probabilities for both pathways

Chart 2

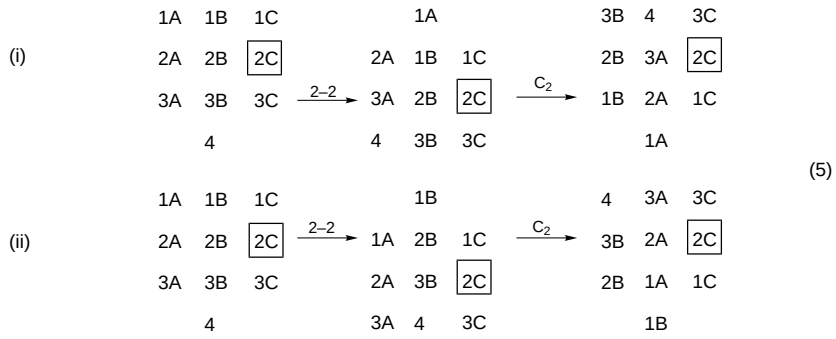

(5)

Table 6. Reduced Exchange Matrices for the Three Dynamic Mechanisms in the Halogeno Bullvalenes Discussed in the Text[a]

(a)

	1A	1B	2A	2B	3A	3B	1C	3C	4	1A′	1B′	2A′	2B′	3A′	3B′	1C′	3C′	4′
1A	−1									1								
1B		−1									1							
2A			−1									1						
2B				−1									1					
3A					−1									1				
3B						−1									1			
1C							−1									1		
3C								−1									1	
4									−1									1
1A′	1									−1								
1B′		1									−1							
2A′			1									−1						
2B′				1									−1					
3A′					1									−1				
3B′						1									−1			
1C′							1									−1		
3C′								1									−1	
4′									1									−1

(b)

	1A	1B	2A	2B	3A	3B	1C	3C	4
1A	−1					.5			.5
1B		−1			.5				.5
2A			−1	.5		.5			
2B			.5	−1	.5				
3A		.5		.5	−1				
3B	.5		.5			−1			
1C							−1	1	
3C							1	−1	
4	.5	.5							−1

(c)

	1A	1B	2A	2B	3A	3B	1C	3C	4	1A′	1B′	2A′	2B′	3A′	3B′	1C′	3C′	4′
1A	−1														.5			.5
1B		−1												.5				.5
2A			−1										.5		.5			
2B				−1								.5		.5				
3A					−1						.5		.5					
3B						−1				.5		.5						
1C							−1										1	
3C								−1								1		
4									−1	.5	.5							
1A′						.5			.5	−1								
1B′					.5				.5		−1							
2A′				.5		.5						−1						
2B′			.5		.5								−1					
3A′		.5		.5										−1				
3B′	.5		.5												−1			
1C′								1								−1		
3C′							1										−1	
4′	.5	.5																−1

[a] The full exchange matrix is obtained by multiplication with an appropriate rate constant.

leads to the exchange matrixes (b) and (c) of Table 6. Case (b) corresponds to a 9 × 9 exchange problem, since it involves just one type of molecules (say, the unprimed), with an identical matrix for the other (primed) type. Case (c) is more complicated since the rearrangement also transforms a primed to an unprimed molecule, and the exchange matrix is therefore twice as large. Again the $2C^2$ carbons are not included: they would be represented by isolated blocks in the exchange matrixes and are at any rate not observed in the experiments.

As indicated above, the slow exchange limit MAS spectra are not sensitive enough to distinguish between the various possible mechanisms depicted in Figure 10. A distinction can, however, be made by using suitable 2D exchange experiments, such as the rotor-synchronized MAS version, developed by Veeman[22] and by Spiess and co-workers.[23−25] In such experiments pure reorientations are manifested by auto cross-peaks between spinning sidebands of the same nuclear species, while chemical exchange results in hetero cross-peaks, which link sidebands of different nuclear species. Experimental rotor synchronized 2D exchange spectra of bromobullvalene recorded at −25 °C (ν_R = 3.0 kHz) at three different mixing times are shown in the left column of Figure 11. It may be seen that with increasing mixing time there is a gradual increase in the intensity of the cross-peaks. Both auto and hetero cross-peaks show up, but the latter appear first, thus providing a clear indication that the dominant mechanism responsible for the dynamic effects involves bond shift rearrangement and not pure π-flips. We can thus rule out mechanism (a) of Figure 10, since such a mechanism would only yield auto cross-peaks.

To check whether the bond shift process corresponds to

mechanism (b) or (c) we need to compare the experimental 2D spectra of Figure 11 with simulations computed for the two mechanisms (exchange matrixes (b) and (c) in Table 6). Procedures for calculating such 2D exchange spectra are discussed in refs 1, 2, and 21−23. Using chemical shift tensors from Table 5 with the orientations shown in Figure 8 and the geometries assumed in Figure 10, two sets of 2D exchange spectra were calculated for different $k_\alpha\tau_m$ values, where $\alpha \equiv$ b, c for mechanisms b and c, respectively. The simulated spectra are shown in the right (mechanism b) and middle (mechanism c) columns of Figure 11. Although the patterns in the two sets of spectra are similar, there are conspicuous differences. In particular, for mechanism (b) the hetero cross-peaks linking the (1AB) carbons with the olefinic carbons grow at a similar rate as those linking the latter with the (1C,4) carbons, while for mechanism (c) the intensity of the former cross-peaks increases faster with the mixing time than the latter. Examination of the experimental spectra (left column) clearly shows that they fit better mechanism (c). We thus conclude that the dominant dynamic process in bromobullvalene involves a bond shift rearrangement leading, at the same time, to inversion of the molecular orientation. The bond shift rearrangement and the dynamic orientational disorder in this compound are thus one and the same process, as the Cope rearrangement effectively also flips the molecule. This result is perhaps not surprising: Referring to Figure 10 we note that in mechanism (c) there is very little displacement of atoms within the void occupied by the bromobullvalene molecule, while mechanisms (a) and (b) require a real reorientation of the whole molecule, which is apparently strongly hindered by the packing forces of the lattice.

Now, that the mechanism of the dynamic process has been established, we can quantitatively analyze the dynamic MAS spectra of the type shown in Figure 9, by comparison with simulated line shapes. Procedures to calculate such spectra are described in refs 26, 1, 2, and 14. Following a suggestion by S. Vega we simplified our earlier procedure[14] of calculating the dynamic MAS spectra as briefly discussed below.

We start with eqs 14 and 19 of ref 14, which give the contribution to the MAS FID of the nuclei in site i

$$M^i(t) = \sum_j U_{ij}(t)P^j = \sum_j [\sum_n \langle in|\exp(-iH_F t)|j0\rangle \times \exp(in\omega_R t)]P^j = \sum_{j,n,g,p} [\langle in|D|gp\rangle \exp(-i\lambda_p^g t)\langle gp|D^{-1}|j0\rangle \times \exp(in\omega_R t)]P^j \quad (6)$$

In this equation H_F is the Floquet Hamiltonian, D is the matrix of eigenvectors which diagonalizes H_F, λ_p^g are its eigenvalues, i, j, and g are indices labeling the sites, P^j are equilibrium populations, and n and p label the Floquet states. In our previous computational procedure we carried out the full two-dimensional product over the indices, g and p, which resulted in excessive computer time. Recalling that the eigenvalues of H_F are periodic[26]

$$\lambda_p^g = \lambda_{p-k}^g + k\omega_R \quad (7)$$

and that the eigenvectors are related by shifts in the Floquet indices

$$\langle gp|D|jq\rangle = \langle G(p-k)|D|J(q-k)\rangle \quad (8)$$

we can rewrite eq 6 in terms of just the principal eigenvalues, λ_0^g, as follows

$$M^i(t) = \sum_{j,n,g,p} [\exp[i(n-p)\omega_R t]\langle i(n-p)|D|g0\rangle \times \exp(-i\lambda_0^g t)\langle g0|D^{-1}|j(-p)\rangle]P^j \quad (9)$$

Changing the summation indices n to $n-p$ and p to $-p$ (both are dummy indices which vary from $-\infty$ to ∞) and renaming them n and p, respectively, eq 9 becomes

$$M^i(t) = \sum_{j,g,n,p} []P^j \rightarrow \sum_{j,g,(n-p),-p} []P^j \rightarrow \sum_{j,g,n,p} [\exp(in\omega_R t)\langle in|D|g0\rangle \exp(-i\lambda_0^g t)\langle g0|D^{-1}|jp\rangle]P^j = \sum_{g,n} \exp(in\omega_R t)\langle in|D|g0\rangle \exp(-i\lambda_0^g t)A_g \quad (10)$$

where

$$A_g = \sum_{j,p} \langle g0|D^{-1}|jp\rangle P^j \quad (11)$$

We thus need to compute the sum over p only once with a considerable saving in computation time. The principal eigenvalues, λ_0^g, are identified as those appearing in the range $-{}^1/_2\omega_R$ to $+{}^1/_2\omega_R$ in the computer output of eigenvalues. Otherwise the calculations were carried out as explained before.[14]

Calculated dynamic spectra for bromobullvalene, which fit best the experimental results are shown in the right columns of Figure 9. For these simulations we need to assume for each line a line width ($\Delta = 1/\pi T_2$) and an effective cross polarization efficiency (CP_{eff}). In practice the anisotropic chemical shift tensors of the aliphatic carbons had negligible effect on the calculated spectra and were therefore neglected in the simulations. These parameters are included in Table 5. The derived Arrhenius plot for the rate constant k_c is given in Figure 12 (here the subscript refers to mechanism c of Figure 10). This plot also includes rate constants derived at low temperatures from the 2D spectra and from 1D magnetization transfer experiments. In the latter experiments the evolution of the spectrum after inverting the aliphatic peaks was monitored and analyzed in terms of both k_c and the longitudinal relaxation time T_1.[1] The latter, however, has only a minor effect on the results: its value changes from about 14 min at −30 °C to ∼11 min at room temperature, which is much longer than the k_c^{-1} in the corresponding temperature range.

The results for iodobullvalene are very similar to those of bromobullvalene. Two-dimensional exchange experiments gave patterns similar to those for the bromo homologue, indicating that mechanism (c) of Figure 10 is also the dominant mechanism responsible for the dynamic line broadening effects in iodobullvalene. Simulated 1D dynamic spectra fitted to the experimental results are included in Figure 9, and the derived rate constants, k_c, are plotted in Figure 12. A summary of the kinetic parameters for both bromo- and iodobullvalene is given in Table 7.

E. Carbon-13 MAS NMR Spectra of Solid Chlorobullvalene. As indicated above chlorobullvalene is liquid at room temperature, and it can be solidified in the NMR probe by cooling to well below its freezing point. The carbon-13 MAS spectra of this solid exhibit relatively sharp peaks due to both isomers 2 and 3, which remain unbroadened by dynamic effects up to its melting. We can nevertheless obtain some dynamic information on this solid from rotor-synchronized 2D exchange spectra as discussed above for bromo- and iodobullvalene. Such

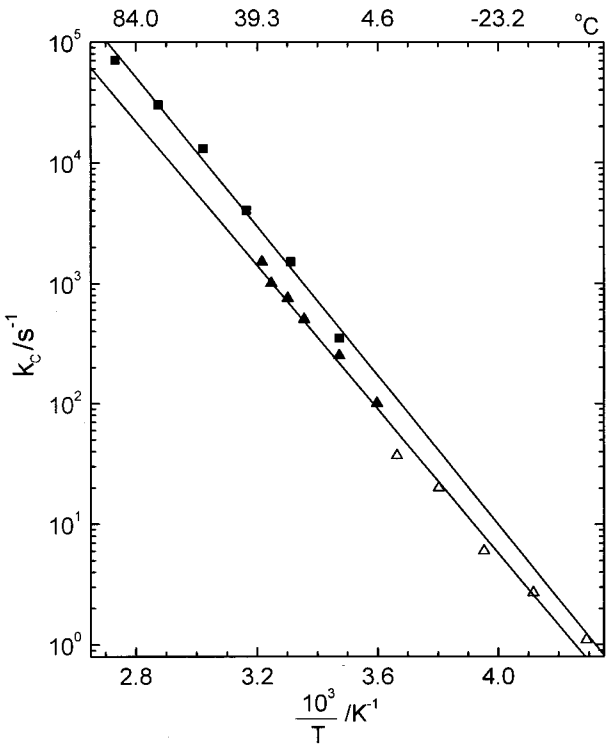

Figure 12. Arrhenius plots for the k_c rate constants in bromo (triangles) and iodobullvalene (squares). The solid symbols are experimental results from dynamic MAS spectra. The open symbols are from magnetization transfer experiments.

Table 7. Kinetic Parameters for the Degenerate Rearrangement, k_c, in Solid Bromo- and Iodobullvalene[a]

X	A/s^{-1}	$\Delta E_c^{\dagger}$/kJ mol^{-1}	$\Delta S_c^{\dagger}$/eu	k_c (300 K)/s^{-1}
Br	5.2×10^{12}	57.1 ± 8.5	-2.4 ± 7.5	0.59×10^3
I	1.8×10^{13}	58.5 ± 5.9	0.1 ± 4.3	1.17×10^3

[a] $k_c = A \exp(-\Delta E^{\dagger}/RT) = (ek_BT/h) \exp(\Delta S_c^{\dagger}/R) \exp(-\Delta H_c^{\dagger}/RT)$.

a spectrum is shown in Figure 13. It was recorded at 125.7 MHz at −8 °C, with $\nu_R = 7.5$ kHz and a mixing time $\tau_m = 3$ s. Note that in the corresponding 1D spectrum shown at the top of the figure, the 4^3 and $1C^2$ peaks are structureless, unlike in the chlorobullvalene spectrum shown in Figure 7, which was recorded at 75.46 MHz. Apparently, at the higher field used for this experiment the effect of the chlorine quadrupole coupling becomes negligible. In the 2D exchange spectrum a large number of hetero cross-peaks are observed indicating the occurrence of bond shift rearrangement. However, a close examination of the resolved regions in the 2D pattern shows that there are no exchange cross-peaks which link signals of isomer 2 with those of isomer 3. The interconversion between these isomers may be described by diagrams as shown in eq 2 for solution and would result in cross-peaks linking the signal of $1C^2$ with 4^3 and that of 4^2 with $1C^3$. Such cross-peaks are clearly missing in the 2D pattern of Figure 13 (see dashed connectivity lines). On the other hand the 4^2 signal shows a conspicuous cross-peak with that of $1AB^2$ and the $1C^2$ signal with $3C^2$ (solid connectivity lines in Figure 13), as would be expected for the degenerate $2 \leftrightarrows 2$ rearrangement (see eq 5). Similarly the 4^3 signal shows a cross-peak with that of $3AB^3$, while $1C^3$ exhibits no cross-peaks at all. This behavior is consistent with the pseudodegenerate cycle $3 \rightarrow [1] \rightarrow 3$, as discussed for the solution spectra (see k_{33}^1 entries in Table 2). We thus conclude that in the solidified sample of chlorobullvalene, which contains both isomers 2 and 3, there is no interconversion between the two isomers, but each one undergoes a degenerate (or pseudodegenerate) rearrangement. The distinct cross-peak linking the 4^2 signal with that of the olefinic carbons must, on the basis of the above conclusions, be attributed to a second order (two-steps) exchange corresponding to the sequence $4^2 \rightarrow 1AB^2 \rightarrow 3AB^2$. The rate constants for these processes, based on magnetization transfer experiments at 270 °C, are about 3 s^{-1} (with $T_1 = 26$ min). This value is about a factor 20 lower than k_c for the bromo and iodo derivatives at the same temperature (cf. Figure 12).

The question concerning the nature of the chlorobullvalene solid, measured in these MAS experiments, remains open. One possibility is that upon cooling the liquid in the NMR rotor a glass is formed, which preserves the isomeric consistency of liquid chlorobullvalene. Differential scanning calorimetry measurements show that fast cooling (>5 K/min) indeed result in a glass formation, as evidenced by a sigmoid in the thermogram at about −95 °C. Upon heating, one usually observes a crystallization (exothermic) peak around −40 °C and always a sharp melting at 14 °C with essentially the same enthalpy (of 13.5 kJ/mol). Similarly, when bromobullvalene was melted in the spinner of the MAS probe and then rapidly solidified by cooling the same spectrum was observed as for the solution-crystallized sample. We therefore believe that the chlorobullvalene measured in our MAS experiment was not a glass form. Also, in such a case we would expect to observe a $2 \leftrightarrows 3$ interchange, as was found in solution.

A second possibility is that the two isomers segregate and crystallize separately, so that the sample consists of a mixture of two types of crystals due to isomer 2 and isomer 3, respectively. In each type of crystals the isomers undergo degenerate (or pseudodegenerate) rearrangement, so that no interchange between isomers 2 and 3 takes place. Finally, it is also possible that chlorobullvalene solidifies as a mixed crystal with specific sites for isomer 2 and others for isomer 3. In such a case we would expect a stoichiometric ratio for the two isomers. This is not inconsistent with the experimental results, which, on the basis of the peak intensities gave approximately a 1:1 molar ratio of the two isomers. In this situation each isomer can undergo a degenerate (or pseudodegenerate) rearrangement which preserves the crystal stoichiometry and structure. Our NMR experiments, however, cannot distinguish between the various possibilities. We hope that an X-ray structure determination will provide an answer to this question.

Summary and Conclusions

Chloro-, bromo-, and iodobullvalene in solution exist predominantly as isomers 2 and 3 and undergo thermally activated bond shift rearrangement. The dominant mechanisms of this rearrangement involve the interconversion of isomers 2 and 3, the degenerate rearrangement of isomer 2, and the pseudodegenerate rearrangement of isomers 3 (via isomer 1, as an intermediate).

In the solid state, bromo- and iodobullvalene crystallize entirely in the form of isomer 2. Their lattices (*Fdd*2) are well ordered but the molecules are orientationally disordered. The disorder is dynamic and, at around room temperature and above, it falls in the range of the NMR time scale. It is shown that this dynamic disorder is coupled with the degenerate Cope rearrangement of isomer 2. In this process the heavy halogen atom (Br, I) remains essentially fixed, while the bond shift process moves around the lighter carbon atoms. Their displacement during this coupled orientational disorder/bond shift rearrangement is small and essentially unhindered by the crystal forces. Consequently the kinetic parameters for this process

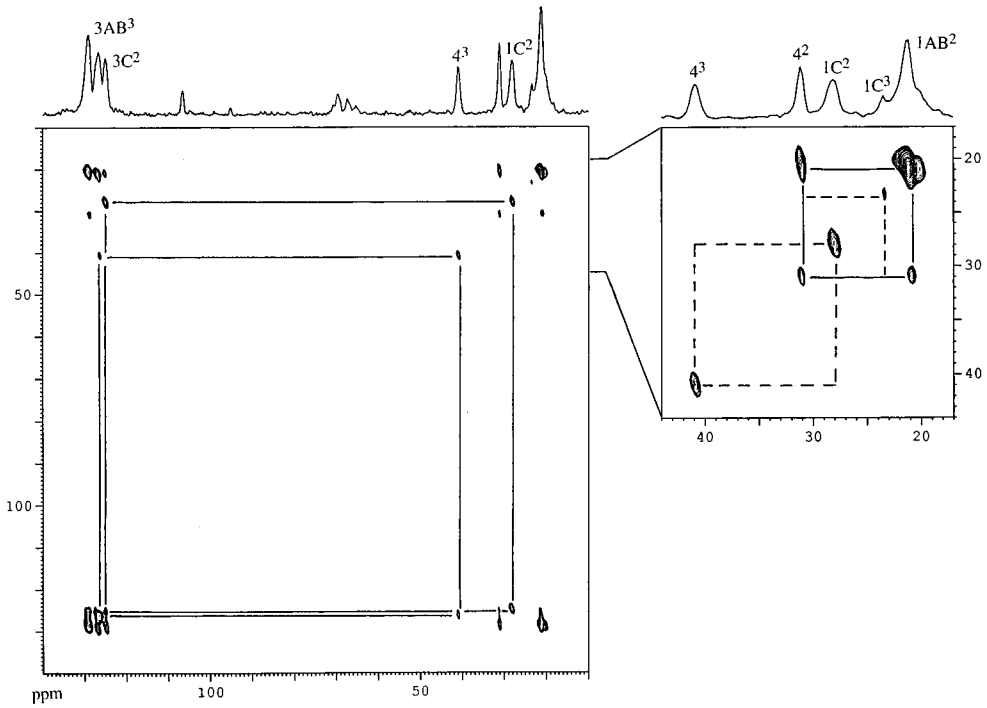

Figure 13. Rotor-synchronized carbon-13 2D exchange spectra for solid (frozen) chlorobullvalene at 125.7 MHz, $t = -8$ °C, $\nu_R = 7.5$ kHz. Phase sensitive spectra with 75 t_1 increments spaced at 33.3 μs with eight scan for each t_1 point, were recorded. Recycle time, 3 min. The vertical and horizontal solid and dashed lines emphasize respectively existing or missing cross-peaks between well resolved signals of isomers 2 and 3.

are very similar to those for the bond shift rearrangement in solution (cf. Tables 3 and 7). The situation is similar to that for unsubstituted bullvalene, where it was found that the rate of the Cope rearrangement in the solid state and in solution are similar.[14,27] In the latter case a reorientation, concomitant with the rearrangement, is required in order to retain the crystal order. However, there is, apparently, little hindrance by the lattice forces on the "soft" transition state from doing so. For monosubstituted bullvalenes, where the substitution sites are at positions 3 (for example for X = CN, COOH) or 4 (X = F), the situation is different. In these cases no degenerate rearrangement is possible, and the bond shift process must proceed via well-defined isomeric species (isomer 1 in the former[2] and isomers 3 and 1 in the latter[1]). This situation leads to a large negative activation entropy and thus to a low preexponential factor. Consequently, although the activation energies for the rearrangement in solution[12] and in the solid state[1,2] of these compounds are similar, the rate of the process is much slower in the crystalline state than it is in the liquid.

Acknowledgment. We thank Professor Shimon Vega for helpful discussion concerning the computation of the dynamic MAS spectra and Professor Gerhard Schröder for advice concerning the preparative aspects of the compound studied. This research was supported by a Grant from GIF, the German-Israeli Foundation for Scientific Research and Development and by the G.M.J. Schmidt Minerva Center on Supramolecular Architectures. K.H. thanks the Fonds der Chemischen Industrie for financial support.

JA9728029